

## Spin Hall Effects Due to Phonon Skew Scattering

Cosimo Gorini

*Institut für Theoretische Physik, Universität Regensburg, 93040 Regensburg, Germany*

Ulrich Eckern

*Institut für Physik, Universität Augsburg, 86135 Augsburg, Germany*

Roberto Raimondi

*Dipartimento di Matematica e Fisica, Roma Tre University, Via della Vasca Navale 84, 00146 Rome, Italy*

(Received 14 January 2015; published 14 August 2015)

A diversity of spin Hall effects in metallic systems is known to rely on Mott skew scattering. In this work its high-temperature counterpart, phonon skew scattering, which is expected to be of foremost experimental relevance, is investigated. In particular, the phonon skew scattering spin Hall conductivity is found to be practically  $T$  independent for temperatures above the Debye temperature  $T_D$ . As a consequence, in Rashba-like systems a high- $T$  linear behavior of the spin Hall angle demonstrates the dominance of extrinsic spin-orbit scattering only if the intrinsic spin splitting is smaller than the temperature.

DOI: [10.1103/PhysRevLett.115.076602](https://doi.org/10.1103/PhysRevLett.115.076602)

PACS numbers: 72.25.-b, 72.10.Di

The spin Hall effect (SHE) [1–5] is the generation of a transverse spin current by an applied electric field, the spin current polarization being perpendicular to both current and field directions. Indeed, a family of related effects exists [6]. The SHE and its inverse are routinely employed in spin injection or extraction experiments in a variety of systems [7–13], and their potential for spintronics applications is becoming ever more evident [14]. A crucial issue is the determination of the dominant spin-orbit mechanism responsible for such effects. In particular, whether this is of *intrinsic* origin, i.e., connected with the band and/or device structure or geometry, or *extrinsic*, i.e., due to impurities. Spin-orbit phenomena are typically complex in their own right, mixing charge and spin (magnetic) degrees of freedom in a plethora of ways, and standard experimental setups add to such a complexity [15]. We will see that one of the main phenomenological arguments employed to discern the dominant spin-orbit mechanism misses the central aspect of dynamical spin-orbit interaction. The latter describes *inter alia* the direct interaction between the electrons' spin and phonons, and, though it will be the leading process at experimental temperatures  $T \approx 300$  K, it has been mostly neglected until now [16].

At  $T = 0$  in metallic systems there are three main *extrinsic* spin-orbit mechanisms: (i) side-jump [17], (ii) skew scattering [18], and (iii) Elliott-Yafet spin relaxation [19]. When a charge current is driven through a sample, (i) and (ii) give rise to a transverse spin current via the side-jump and skew scattering spin Hall conductivities, denoted  $\sigma_{sj,0}^{sH}$  and  $\sigma_{ss,0}^{sH}$ , respectively. Elliott-Yafet spin relaxation is typically weak, but is needed to ensure the proper analytical behavior of the full spin Hall conductivity  $\sigma^{sH}$  when also *intrinsic* spin-orbit interaction is present—as

is the case in thin films or two-dimensional (2D) electron or hole gases [20].

The above mechanisms have been extensively studied at  $T = 0$ , where they arise from electron scattering at static impurities. In this case one has (explicitly in 2D) [21]

$$\sigma_{sj,0}^{sH} = \frac{en}{\hbar} \left(\frac{\lambda}{2}\right)^2, \quad \sigma_{ss,0}^{sH} = \left(\frac{\lambda k_F}{4}\right)^2 \frac{en}{m} 2\pi N_0 v_0 \tau_0 \quad (1)$$

with  $n$  the electron density,  $\lambda$  the effective Compton wavelength of extrinsic spin-orbit coupling,  $v_0$  the scattering amplitude,  $k_F$  the Fermi wave vector,  $N_0 = m/2\pi\hbar^2$  the density of states,  $\tau_0$  the elastic scattering time, and  $e > 0$  the unit charge. Equation (1) shows that the side-jump conductivity is independent of the scattering mechanism (at least in simple parabolic bands), whereas the skew scattering one is proportional to  $\tau_0$ , i.e., to the Drude conductivity  $\sigma_D = e^2 n \tau_0 / m = -en\mu$  ( $\mu = -e\tau_0/m$  is the mobility). From these  $T = 0$  results, the  $T \neq 0$  spin Hall conductivity behavior is extrapolated arguing that the skew scattering conductivity should behave as  $\sigma_{ss}^{sH} \propto \mu$ , with the proportionality constant depending on microscopic details (impurity concentration,  $k_F$ , etc.), but *not* on the temperature. Hence, the argument goes as follows [8,10,13,22,23]: (i) in high mobility samples skew scattering should dominate, and (ii) the spin Hall signal should scale as the mobility with respect to its  $T$  dependence. On the contrary, the same signal should be  $T$  independent in samples where the side-jump mechanism is the leading one.

However, we will see that this simple and appealing phenomenological extrapolation from  $T = 0$  to  $T \neq 0$  misses a critical feature of high- $T$  skew scattering—which, following Ref. [13], we call “phonon skew scattering.”

Namely, that for temperatures  $T \gtrsim T_D$ , with  $T_D$  the Debye temperature,  $\sigma_{ss}^{sH}$  does *not* scale as the mobility and rather becomes  $T$  independent. Since typical spin Hall experiments are performed at room temperature in “soft” metals such as Au ( $T_D = 165$  K), Pt ( $T_D = 240$  K), or Ta ( $T_D = 240$  K) [8,11,24], this makes distinguishing between side-jump and skew scattering contributions an even more complicated issue.

The Hamiltonian is (compare Ref. [16])

$$H = H_0 + \delta V^{\text{ph}}(\mathbf{r}, t) - \frac{\lambda^2}{4\hbar} \boldsymbol{\sigma} \times \nabla \delta V^{\text{ph}}(\mathbf{r}, t) \cdot \mathbf{p} + H_1^{\text{ph}}, \quad (2)$$

where  $\boldsymbol{\sigma}$  is the vector of Pauli matrices. Here  $H_0$  contains the static electronic part of the Hamiltonian, in first-quantized notation given by

$$H_0^{\text{el}} = \frac{p^2}{2m} - \frac{\alpha}{\hbar} \boldsymbol{\sigma} \times \hat{\mathbf{z}} \cdot \mathbf{p} + V_{\text{imp}}(\mathbf{r}) - \frac{\lambda^2}{4\hbar} \boldsymbol{\sigma} \times \nabla V_{\text{imp}}(\mathbf{r}) \cdot \mathbf{p}, \quad (3)$$

as well as the standard harmonic phonon contribution:  $H_0 = H_0^{\text{el}} + H_0^{\text{ph}}$ . The second term on the rhs of Eq. (3) is a Bychkov-Rashba-like intrinsic spin-orbit term [25], which appears at the interface between transition metals and insulators or vacuum where inversion symmetry is broken [26]. The potential from static impurities is denoted  $V_{\text{imp}}(\mathbf{r})$ , and  $\delta V^{\text{ph}}(\mathbf{r}, t)$  stands—classically speaking—for the time-dependent potential due to lattice vibrations at  $T \neq 0$ .

The actual calculations employ well-known quantum field theoretical techniques, see below. Here we only mention that it is convenient to introduce the phonon field operator [27]

$$\hat{\varphi}(\mathbf{r}) = i \sum_{\mathbf{k}} \sqrt{\frac{v_s k}{2V}} (\hat{b}_{\mathbf{k}} e^{i\mathbf{k}\cdot\mathbf{r}} - \text{c.c.}), \quad (4)$$

where  $\hat{b}_{\mathbf{k}}$  and  $\hat{b}_{\mathbf{k}}^\dagger$  are annihilation and creation operators for longitudinal Debye phonons of momentum  $\hbar\mathbf{k}$ ,  $v_s$  is the sound velocity, and  $V$  the volume (or the area in 2D). Note that  $\hat{\varphi}(\mathbf{r})$  corresponds to  $v_s \sqrt{\rho}$  times the divergence of the ionic displacement, where  $\rho$  is the ionic mass density. As usual, the electron-phonon coupling constant will be denoted by  $g$  [27]. Finally, the anharmonic term (3-phonon processes) reads

$$H_1^{\text{ph}} = \frac{\Lambda}{3!} \int d\mathbf{r} \hat{\varphi}^3(\mathbf{r}). \quad (5)$$

In its most general form, there appears a tensor arising from the third derivatives of the crystal potential with respect to small displacements [28]. For our purposes, however, it is sufficient to characterize the anharmonicity by the single

parameter  $\Lambda$ , which is related to the Grüneisen parameter  $\gamma$  by  $\Lambda = -\gamma/\rho^{1/2}v_s$ ; typically  $\gamma \approx 2 \dots 3$  [28].

The  $T = 0$  processes, as well as the dynamical side-jump and Elliott-Yafet processes, have been discussed in Ref. [16]. In particular, skew scattering from impurities is described by the self-energy diagrams of Fig. 1(b), together with the self-energy (a1) yielding the self-consistent Born approximation for the elastic scattering time. In order to study finite (high) temperatures, the self-energy (a2) as well as the skew-scattering from phonons via the self-energy diagrams of Fig. 1(c) have to be taken into account.

Just as for the second order self-energies [Fig. 1(a)], there is a direct correspondence between the diagrams due to impurities [Fig. 1(b)] and those due to phonon scattering [Fig. 1(c)]. Such a correspondence appears in the high-temperature limit, where the phonon dynamics become irrelevant, roughly speaking  $\hat{\varphi}(\mathbf{r}, t) \rightarrow \varphi(\mathbf{r})$  [29]. To illustrate this further, consider diagrams of Fig. 1(b), with the impurity potentials—before averaging—replaced by the classical phonon field  $g\varphi(\mathbf{r})$ . The average is then performed using the equipartition law

$$\langle \varphi(\mathbf{r}_1) \varphi(\mathbf{r}_2) \rangle_T = k_B T \delta(\mathbf{r}_1 - \mathbf{r}_2), \quad (6)$$

where  $\langle \dots \rangle_T$  denotes the classical average, and

$$\langle \varphi(\mathbf{r}_1) \varphi(\mathbf{r}_2) \varphi(\mathbf{r}_3) \rangle_T = -\Lambda (k_B T)^2 \delta(\mathbf{r}_1 - \mathbf{r}_2) \delta(\mathbf{r}_1 - \mathbf{r}_3) \quad (7)$$

which follows from expanding the Boltzmann factor to first order with respect to the anharmonic term. In the case of impurity scattering, the equivalent of the rhs of Eq. (6), assuming “white-noise” disorder, is given by  $n_i v_0^2 \delta(\mathbf{r}_1 - \mathbf{r}_2)$ , while the three-field average results in  $n_i v_0^3 \delta(\mathbf{r}_1 - \mathbf{r}_2) \delta(\mathbf{r}_1 - \mathbf{r}_3)$ . This suggests that one can obtain the high- $T$  results through the following correspondence:

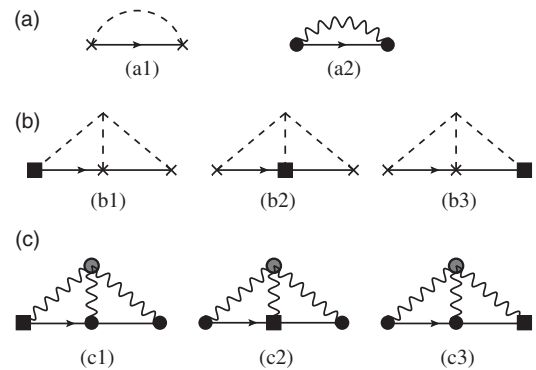


FIG. 1. (a) Self-energy in the standard self-consistent Born approximation for electron-impurity (a1) and electron-phonon (a2) scattering. (b) Diagrams describing skew-scattering from impurities, and (c) diagrams describing skew-scattering from phonons. Dashed and wiggly lines indicate the impurity average and phonon propagator, respectively. The square box is the spin-orbit insertion due to both impurity and phonon potential.

$$n_i v_0^2 \rightarrow g^2 k_B T = \frac{1}{2\pi N_0 \tau} \quad (8)$$

$$n_i v_0^3 \rightarrow -\Lambda g^3 (k_B T)^2 = \frac{1}{2\pi N_0 \tau} (-k_B T g \Lambda). \quad (9)$$

Note that  $\tau$  here denotes the  $T$ -dependent electron-phonon scattering time, in contrast to  $\tau_0$  due to elastic scattering from impurities;  $-1/2\tau$  corresponds to the imaginary part of the retarded self-energy as derived from (a2), with the result given in Eq. (8) [28]. Using Eqs. (8) and (9) in Eq. (1), the skew-scattering conductivity reads

$$\sigma_{ss}^{sH} = -\left(\frac{\lambda k_F}{4}\right)^2 \frac{en \hbar \Lambda}{m g}, \quad (10)$$

which is, in particular,  $T$  independent. Thus the  $T$  dependence of the spin Hall conductivity must interpolate between the two limiting expressions at low [see Eq. (1)] and high [see Eq. (10)] temperature.

In order to compare the order of magnitude of the two limits, we use the standard relations valid for an isotropic metal,  $v_0 \sim 1/2N_0$  (screened Coulomb impurities),  $g^2 \sim 1/2N_0$ ,  $\rho v_s^2 \sim N_0 \epsilon_F^2$ . For the ratio between the high- and low- $T$  conductivities we thus obtain

$$\frac{\hbar \Lambda}{g\tau} \sim \frac{\gamma}{\epsilon_F \tau_0} \sim 0.1, \quad (11)$$

where, to be explicit, we assumed  $\epsilon_F \tau_0 / \hbar \approx 20$ . Note, however, that there might be a sign change as a function of temperature, depending on the nature of the impurities, i.e., the sign of  $v_0$ , as well as on the sign of  $g$ .

A quantum field theoretical (Keldysh) calculation confirms the above results up to a numerical prefactor in Eq. (9). Besides providing a solid basis for what has been obtained through simple and intuitive arguments, we stress that such a calculation is necessary in order to study the full temperature range  $0 < T < T_D$ .

We now outline the Keldysh calculation in the high- $T$  regime, where the self-energy diagrams of Fig. 1(c) acquire a transparent form [30]. In fact it is sufficient to consider the first one (now  $\hbar = k_B = 1$ ):

$$(c1): \Sigma_{ss,13}^T = -\frac{\lambda^2}{4} \Lambda g^3 \sum_{i,j,k} \epsilon_{ijk} \sigma_j (-i\nabla_1^G)_i (\nabla_1^D)_k \times \int_{2,4} G_{12} D_{14} D_{24} D_{34} G_{23}. \quad (12)$$

Here the  $G$ 's are  $SU(2)$ -covariant electron propagators [16,31,32], while the  $D$ 's are free phonon propagators, both defined on the Keldysh contour. The arguments, written as subscripts, include both space and time, e.g.,  $1 = (\mathbf{r}_1, t_1)$ . The notation  $\nabla_1^G$  indicates that the gradient acts only on the

following  $G$  function, and similarly for  $\nabla_1^D$ . After analytical continuation [33], the  $t$  integrals run from  $-\infty$  to  $+\infty$ , and the Keldysh structure is carried by the  $R, A, K$  propagator components. In the high- $T$  regime,  $T \gtrsim T_D$ , we use  $D^< \approx D^> \approx \frac{1}{2} D^K$  [34], with the result

$$(c1): [\Sigma_{ss,13}^T]^{<(>)} = -\frac{\lambda^2}{4} \sum_{i,j,k} \epsilon_{ijk} \sigma_j (-i\nabla_1^G)_i (\nabla_1^D)_k \times \int_2 (G_{12}^R G_{23}^{<(>)} + G_{12}^{<(>)} G_{23}^A) \mathbb{D}_{123}, \quad (13)$$

where

$$\mathbb{D}_{123} = \frac{\Lambda g^3}{4} \int_4 [D_{14}^R D_{24}^K D_{34}^K + D_{14}^K D_{24}^R D_{34}^K + D_{14}^K D_{24}^K D_{34}^R]. \quad (14)$$

Equation (13) has the standard form due to the coupling to an external field, whose role is here played by  $\mathbb{D}$ . Exploiting the fact that the phonon frequencies ( $\sim \omega_D$ ) are small compared to  $\omega \sim T$ , which physically means that electron-phonon scattering is elastic, we obtain

$$\mathbb{D}_{123} \approx -3\Lambda g^3 (k_B T)^2, \quad (15)$$

having restored here  $k_B$  for easy comparison with Eq. (9). The only difference with the latter is a factor of 3, missed by the simple introductory argument. The correct  $T = 0 \rightarrow T > T_D$  correspondence for skew scattering thus reads

$$n_i v_0^3 \rightarrow -3\Lambda g^3 (k_B T)^2. \quad (16)$$

This yields at once

$$\sigma_{ss}^{sH} = -3 \left(\frac{\lambda k_F}{4}\right)^2 \frac{en \hbar \Lambda}{m g}, \quad (17)$$

which is the central result of our work. Apart from the already mentioned factor of 3, it confirms the heuristically obtained Eq. (10), and shows that the skew scattering conductivity at high temperatures does not scale as the mobility, being rather  $T$  independent.

We stress that the current interpretation of (inverse) spin Hall experiments is, however, based on the ‘‘scaling-as-mobility’’ assumption [8,10,13,22,23]. Equation (17) shows that a more careful analysis seems to be required, and has important consequences for the spin Hall angle  $\theta^{sH} \equiv e\sigma^{sH}/\sigma_D$ . As shown in Fig. 2, the spin motion becomes diffusive for  $\Delta < \hbar/\tau \sim k_B T \sim 10^{-2}$  eV and ballistic for  $\Delta > k_B T$ , with  $\Delta = 2\alpha k_F$  the intrinsic splitting. If a nonlinear or decreasing behavior of  $\theta^{sH}$  is observed, we deduce that  $k_B T > \Delta$  and  $(\sigma_{sj}^{sH} + \sigma_{ss}^{sH})/(e/8\pi\hbar) \ll 1$  (extrinsic effects are much weaker than the intrinsic ones).

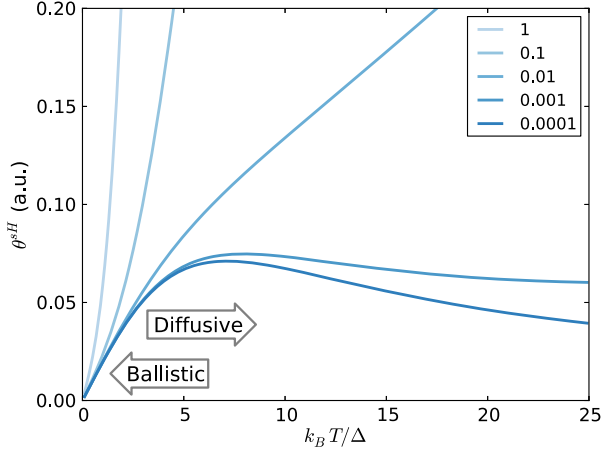


FIG. 2 (color online). Qualitative plot of the  $T > T_D$  spin Hall angle  $\theta^{sH}$  as a function of  $k_B T$ , measured in units of the intrinsic spin-orbit splitting, for the paradigmatic case of a Rashba-like system. The spin Hall conductivity is given by Eq. (19), and we set  $\lambda/\lambda_F \approx 10^{-1}$  [16]. Darker (lighter) curves are for weaker (stronger) extrinsic conductivities,  $(\sigma_{sj}^{sH} + \sigma_{ss}^{sH})/(e/8\pi\hbar) = 10^{-4}, \dots, 1$ .

If, on the other hand, a linear behavior is observed, no conclusion can be reached by simply looking at the  $T$  dependence, since there are two possibilities: (i)  $k_B T > \Delta$  and the extrinsic and intrinsic effects are comparable (light blue curves in Fig. 2); (ii)  $k_B T < \Delta$  and nothing can be said about the relative strength of extrinsic and intrinsic mechanisms (all curves, i.e., for different parameter values, look the same).

The relative importance of phonon vs impurity skew scattering is obtained by comparing the self-energies (b1) and (c1), yielding

$$\Sigma_{ss}^T/\Sigma_{ss}^0 \sim -\gamma(\tau_0/\tau)(k_B T/\epsilon_F). \quad (18)$$

In a metal at room temperature we have  $k_B T/\epsilon_F \sim 10^{-2}$ , setting as threshold for the dominance of phonon skew scattering  $\tau_0 \gtrsim 10^2 \tau$ .

In general, the  $T = 0 \rightarrow T > T_D$  correspondence lets us immediately turn known  $T = 0$  results into their  $T > T_D$  counterparts. For example, the full expression for the high- $T$  spin Hall conductivity and current-induced spin polarization [35] due to intrinsic Bychkov-Rashba coupling and extrinsic *dynamical* spin-orbit interaction is structurally identical to the  $T = 0$  expressions appearing in Ref. [32]. Explicitly for a 2D homogeneous bulk system

$$\sigma^{sH} = \frac{1}{1 + \tau_s/\tau_{DP}} (\sigma_{int}^{sH} + \sigma_{sj}^{sH} + \sigma_{ss}^{sH}) \quad (19)$$

where  $\sigma_{int}^{sH} = (e/8\pi\hbar)(2\tau/\tau_{DP})$  is the intrinsic part of the spin Hall conductivity, and

$$\frac{1}{\tau_s} = \frac{1}{\tau} \left( \frac{\lambda k_F}{2} \right)^4, \quad \frac{1}{\tau_{DP}} = \frac{1}{2\tau} \frac{(\Delta\tau/\hbar)^2}{[(\Delta\tau/\hbar)^2 + 1]} \quad (20)$$

are, respectively, the Elliott-Yafet and Dyakonov-Perel spin relaxation rates. Furthermore, the current-induced spin polarization “conductivity,”  $\mathcal{P}$ , is given by

$$\mathcal{P} = -\frac{2m\alpha}{\hbar^2} \frac{1}{1/\tau_s + 1/\tau_{DP}} (\sigma_{int}^{sH} + \sigma_{sj}^{sH} + \sigma_{ss}^{sH}). \quad (21)$$

This phenomenon, together with its inverse [36–38], is intimately related to the spin Hall effect [38,39] and can be similarly exploited for spin-to-charge conversion [36–38].

We conclude by discussing future perspectives and certain limitations of our approach. First, the anharmonic term [Eq. (5)] was handled via an “ $s$ ”-wave approximation, ignoring the tensor structure of  $\Lambda$  as well as any details of the generally anisotropic phonon-phonon coupling; these, however, are not expected to *qualitatively* modify our conclusions concerning the  $T$  dependence. The same is true when other phonon modes are included, provided their typical frequencies are smaller than  $k_B T/\hbar$ .

Second,  $\phi^4$  (and higher) anharmonicities, formally necessary to stabilize the system, could also be considered. These have their  $T = 0$  parallel in the  $T$ -matrix resummation of skew scattering. However, whereas the latter does not add qualitative new features to the physics described by diagrams of Fig. 1(b), higher anharmonicities could. Roughly speaking, any additional phonon line connected to the anharmonic vertex in diagrams of Fig. 1(c) should contribute a further  $k_B T$  factor in the  $T > T_D$  regime, as well as modifying the prefactor of “3” missed by the simple introductory arguments. This would further increase the importance of phonon skew scattering at high  $T$ ’s, possibly implying a  $T$  behavior of  $\sigma_{ss}^{sH}$  opposite to that of the mobility. Indeed, it would be highly desirable to develop a more detailed theory of phonon scattering, in analogy with the  $T = 0$  treatment by Fert and Levy [40], as well as to elucidate the role of umklapp processes.

Third, band nonparabolicities could be relevant since they modify, in particular, the side-jump mechanism, and thus possibly its  $T$  dependence. Finally, and probably most importantly, the intermediate temperature regime,  $0 < T < T_D$ , needs to be properly investigated. We stress that our Keldysh approach gives an expression for the self-energy [Fig. 1(c)] formally valid for all temperatures. However, at lower  $T$ ’s the interplay between interactions, impurity scattering, and phonons can have important consequences [41]. We expect that our results will stimulate further (much needed) work in these directions of highest experimental relevance.

C. G. and U. E. acknowledge financial support from the Deutsche Forschungsgemeinschaft through SFB 689 and TRR 80, respectively.

- [1] M. I. Dyakonov and V. I. Perel, *Phys. Lett.* **35A**, 459 (1971).
- [2] S. Murakami, N. Nagaosa, and S.-C. Zhang, *Science* **301**, 1348 (2003).
- [3] J. Sinova, D. Culcer, Q. Niu, N. A. Sinitsyn, T. Jungwirth, and A. H. MacDonald, *Phys. Rev. Lett.* **92**, 126603 (2004).
- [4] Y. K. Kato, R. C. Myers, A. C. Gossard, and D. D. Awschalom, *Science* **306**, 1910 (2004).
- [5] J. Wunderlich, B. Kaestner, J. Sinova, and T. Jungwirth, *Phys. Rev. Lett.* **94**, 047204 (2005).
- [6] H.-A. Engel, E. I. Rashba, and B. I. Halperin, in *Handbook of Magnetism and Advanced Magnetic Materials*, edited by H. Kronmüller and S. Parkin (Wiley, New York, 2007), Vol. V, pp. 2858–2877.
- [7] S. O. Valenzuela and M. Tinkham, *Nat. Mater.* **442**, 176 (2006).
- [8] L. Vila, T. Kimura, and Y. C. Otani, *Phys. Rev. Lett.* **99**, 226604 (2007).
- [9] O. Mosendz, V. Vlaminck, J. E. Pearson, F. Y. Fradin, G. E. W. Bauer, S. D. Bader, and A. Hoffmann, *Phys. Rev. B* **82**, 214403 (2010).
- [10] Y. Niimi, M. Morota, D. H. Wei, C. Deranlot, M. Basletic, A. Hamzic, A. Fert, and Y. Otani, *Phys. Rev. Lett.* **106**, 126601 (2011).
- [11] M. Obstbaum, M. Härtinger, H. G. Bauer, T. Meier, F. Swientek, C. H. Back, and G. Woltersdorf, *Phys. Rev. B* **89**, 060407(R) (2014).
- [12] M. Weiler, J. M. Shaw, H. T. Nembach, and T. J. Silva, *Phys. Rev. Lett.* **113**, 157204 (2014).
- [13] M. Isasa, E. Villamor, L. E. Hueso, M. Gradhand, and F. Casanova, *Phys. Rev. B* **91**, 024402 (2015).
- [14] L. Liu, C.-F. Pai, Y. Li, H. W. Tseng, D. C. Ralph, and R. A. Buhrman, *Science* **336**, 555 (2012); L. Liu, O. J. Lee, T. J. Gudmundsen, D. C. Ralph, and R. A. Buhrman, *Phys. Rev. Lett.* **109**, 096602 (2012).
- [15] T. Jungwirth, J. Wunderlich, and K. Olejník, *Nat. Mater.* **11**, 382 (2012).
- [16] S. Tölle, C. Gorini, and U. Eckern, *Phys. Rev. B* **90**, 235117 (2014).
- [17] L. Berger, *Phys. Rev. B* **2**, 4559 (1970).
- [18] J. Smit, *Physica (Amsterdam)* **21**, 877 (1955).
- [19] R. J. Elliott, *Phys. Rev.* **96**, 266 (1954); Y. Yafet, *Solid State Physics* (Academic, New York, 1963), Vol. 14.
- [20] R. Raimondi and P. Schwab, *Europhys. Lett.* **87**, 37008 (2009).
- [21] H.-A. Engel, B. I. Halperin, and E. I. Rashba, *Phys. Rev. Lett.* **95**, 166605 (2005); W.-K. Tse and S. Das Sarma, *Phys. Rev. Lett.* **96**, 056601 (2006).
- [22] E. M. Hankiewicz, G. Vignale, and M. E. Flatté, *Phys. Rev. Lett.* **97**, 266601 (2006).
- [23] G. Vignale, *J. Supercond. Novel Magn.* **23**, 3 (2010).
- [24] T. Kimura, Y. Otani, T. Sato, S. Takahashi, and S. Maekawa, *Phys. Rev. Lett.* **98**, 156601 (2007); T. Seki, Y. Hasegawa, S. Mitani, S. Takahashi, H. Imamura, S. Maekawa, J. Nitta, and K. Takanashi, *Nat. Mater.* **7**, 125 (2008); L. Liu, T. Moriyama, D. C. Ralph, and R. A. Buhrman, *Phys. Rev. Lett.* **106**, 036601 (2011); C. Hahn, G. de Loubens, O. Klein, M. Viret, V. V. Naletov, and J. Ben Youssef, *Phys. Rev. B* **87**, 174417 (2013).
- [25] Y. A. Bychkov and E. I. Rashba, *J. Phys. C* **17**, 6039 (1984).
- [26] A. M. Shikin, A. Varykhalov, G. V. Prudnikova, D. Usachev, V. K. Adamchuk, Y. Yamada, J. D. Riley, and O. Rader, *Phys. Rev. Lett.* **100**, 057601 (2008); A. Varykhalov, J. Sánchez-Barriga, A. M. Shikin, W. Gudat, W. Eberhardt, and O. Rader, *Phys. Rev. Lett.* **101**, 256601 (2008); A. G. Rybkin, A. M. Shikin, V. K. Adamchuk, D. Marchenko, C. Biswas, A. Varykhalov, and O. Rader, *Phys. Rev. B* **82**, 233403 (2010).
- [27] A. A. Abrikosov, L. P. Gor'kov, and I. E. Dzyaloshinski, *Quantum Field Theoretical Methods in Statistical Physics* (Pergamon Press, New York, 1965).
- [28] J. M. Ziman, *Electrons and Phonons* (Clarendon Press, Oxford, 1960).
- [29] The time-dependence of  $\hat{\varphi}(\mathbf{r}, t)$  is due to the interaction picture.
- [30] The self-energy [Fig. 1(c)] for arbitrary  $T$ 's is fairly complicated, and will not be discussed here.
- [31] C. Gorini, P. Schwab, R. Raimondi, and A. L. Shelankov, *Phys. Rev. B* **82**, 195316 (2010).
- [32] R. Raimondi, P. Schwab, C. Gorini, and G. Vignale, *Ann. Phys. (Berlin)* **524**, 153 (2012).
- [33] J. Rammer and H. Smith, *Rev. Mod. Phys.* **58**, 323 (1986); J. Rammer, *Quantum Field Theory of Non-equilibrium States* (Cambridge University Press, Cambridge, England, 2007).
- [34] In general  $D^{(\circ)} = [D^K + (-)(D^R - D^A)]/2$ .
- [35] E. L. Ivchenko and G. E. Pikus, *JETP Lett.* **27**, 604 (1978); F. T. Vas'ko and N. A. Prima, *Sov. Phys. Solid State* **21**, 994 (1979); L. S. Levitov, Y. V. Nazarov, and G. M. Éliashberg, *Sov. Phys. JETP* **61**, 133 (1985); A. G. Aronov and Y. B. Lyanda-Geller, *JETP Lett.* **50**, 431 (1989); V. M. Edelstein, *Solid State Commun.* **73**, 233 (1990); S. D. Ganichev, M. Trushin, and J. Schliemann, in *Handbook of Spin Transport and Magnetism*, edited by E. Y. Tsybmal and I. Zutic (Chapman and Hall, London, 2011), pp. 487–497.
- [36] S. D. Ganichev, E. L. Ivchenko, V. V. Bel'kov, S. A. Tarasenko, M. Sollinger, D. Weiss, W. Wegscheider, and W. Prettl, *Nature (London)* **417**, 153 (2002).
- [37] J. C. R. Sánchez, L. Vila, G. Desfonds, S. Gambarelli, J. P. Attané, J. M. D. Teresa, C. Magén, and A. Fert, *Nat. Commun.* **4**, 2944 (2013).
- [38] K. Shen, G. Vignale, and R. Raimondi, *Phys. Rev. Lett.* **112**, 096601 (2014).
- [39] C. Gorini, P. Schwab, M. Dzierzawa, and R. Raimondi, *Phys. Rev. B* **78**, 125327 (2008).
- [40] A. Fert and P. M. Levy, *Phys. Rev. Lett.* **106**, 157208 (2011).
- [41] A. Schmid, *Z. Phys.* **259**, 421 (1973).